Advanced diffusion-weighted MRI metrics detect sex differences in aging among 15,000 adults in the UK Biobank

Katherine E. Lawrence[a], Leila Nabulsi[a], Vigneshwaran Santhalingam[a], Zvart Abaryan[a], Julio E. Villalon-Reina[a], Talia M. Nir[a], Iyad Ba Gari[a], Alyssa H. Zhu[a], Elizabeth Haddad[a], Alexandra M. Muir[a], Neda Jahanshad[a], Paul M. Thompson[a]
[a]Imaging Genetics Center, Mark and Mary Stevens Neuroimaging & Informatics Institute, University of Southern California, Marina del Rey, CA 90292, USA

ABSTRACT

The brain's white matter microstructure, as assessed using diffusion-weighted MRI (DWI), changes significantly with age and also exhibits significant sex differences. Here we examined the ability of a traditional diffusivity metric (fractional anisotropy derived from diffusion tensor imaging, DTI-FA) and advanced diffusivity metrics (fractional anisotropy derived from the tensor distribution function, TDF-FA; neurite orientation dispersion and density imaging measures of intra-cellular volume fraction, NODDI-ICVF; orientation dispersion index, NODDI-ODI; and isotropic volume fraction, NODDI-ISOVF) to detect sex differences in white matter aging. We also created normative aging reference curves based on sex. Diffusion tensor imaging (DTI) applies a single-tensor diffusion model to single-shell DWI data, while the tensor distribution function (TDF) fits a continuous distribution of tensors to single-shell DWI data. Neurite orientation dispersion and density imaging (NODDI) fits a multi-compartment model to multi-shell DWI data to distinguish intra- and extra-cellular contributions to diffusion. We analyzed these traditional and advanced diffusion measures in a large population sample available through the UK Biobank (15,394 participants; age-range: 45-80 years) by using linear regression and fractional polynomials. Advanced diffusivity metrics (NODDI-ODI, NODDI-ISOVF, TDF-FA) detected significant sex differences in aging, whereas a traditional metric (DTI-FA) did not. These findings suggest that future studies examining sex differences in white matter aging may benefit from including advanced diffusion measures.

Keywords: diffusion-weighted MRI, white matter microstructure, diffusion tensor imaging, tensor distribution function, neurite orientation dispersion and density imaging, sex differences, aging, normative reference curves

1. INTRODUCTION

The brain's white matter microstructure significantly changes over the lifespan, with prior work also demonstrating sex differences in the brain's white matter microstructure as measured with diffusion-weighted MRI (DWI)[1,2]. Differences in aging between men and women may contribute to sex differences in the incidence and course of age-related neurodegenerative diseases such as Alzheimer's disease[3,4]. Most DWI studies thus far have used diffusion tensor imaging (DTI) metrics such as fractional anisotropy (FA) to characterize the white matter[5]. However, more recently developed DWI methods such as the tensor distribution function (TDF) and neurite orientation dispersion and density imaging (NODDI) may provide more refined representations of underlying white matter properties[6-10]. DTI applies a single-tensor diffusion model to single-shell DWI data, whereas TDF models multiple underlying fiber populations in single-shell DWI data, and NODDI applies a multi-compartment model to multi-shell DWI data[5-10].

Here we investigated the ability of both traditional diffusion methods (DTI) and advanced diffusion methods (TDF, NODDI) to capture differences in white matter microstructure. We specifically focused on the relative sensitivity of these metrics to sex differences in brain aging, due to the potential relevance of such sex differences to conditions such as Alzheimer's disease. Whole-brain DWI data available through the UK Biobank was analyzed to examine the following diffusivity metrics: DTI-FA, TDF-FA, NODDI-ICVF (intra-cellular volume fraction), NODDI-ODI (orientation dispersion index), and NODDI-ISOVF (isotropic volume fraction). We also created sex-stratified centile reference curves[11-13] for each diffusivity metric to provide normative models of white matter aging among men and women, as such

normative reference values may allow for the future stratification of individuals at risk for age-related neurodegenerative diseases.

2. METHODS

2.1 Data acquisition

The UK Biobank is a publicly available dataset of community-based middle-aged and older adults residing in the United Kingdom[14]. Here we analyzed cross-sectional data from a total of 15,394 UK Biobank participants aged 45-80 years old. Subjects were classified as male or female based on chromosomal sex; participants were only included if their chromosomal sex was identical to their sex as recorded elsewhere in the UK Biobank (i.e., participant sex as reported by the subject or as recorded in the subject's medical records). Our sample consisted of an approximately equal number of males and females (47.63% male, 52.36% female). Whole-brain DWI data was collected on a single Siemens Skyra 3T scanner within this sample using a standard Siemens 32-channel head coil. As detailed elsewhere[14], DWI data were acquired using a spin-echo echo-planar imaging sequence with 5 b=0 s/mm^2 (plus an additional 3 blip-reversed b=0 s/mm^2), 50 b=1000 s/mm^2 and 50 b=2000 s/mm^2 diffusion-weighted volumes, for a total of 100 distinct diffusion-encoding directions. A multiband acceleration factor of 3 was used for acquisition, with a 104x104x72 field of view and a voxel size of 2x2x2 mm. Informed consent was obtained from all participants, and ethical approval for the UK Biobank was received from the research ethics committee. The research reported here was conducted using the UK Biobank Resource under Application Number 11559.

2.2 DWI processing

DWI data were preprocessed as described in Alfaro-Almagro et al.[15] Briefly, eddy currents, head motion, and outlier slices were corrected using FSL's Eddy tool[16,17], and gradient distortion correction was then applied.

Measures derived from single-shell DWI data (b=1000 s/mm^2, 50 gradients) included a traditional single-tensor model of fractional anisotropy (DTI-FA) and an advanced measure of fractional anisotropy derived using the tensor distribution function (TDF-FA), which models multiple underlying fiber populations. DTI-FA was fit using FSL's DTIFIT, and TDF-FA was fit using in-house scripts[8]. Measures derived from the multi-shell DWI data (b=1000 s/mm^2, b=2000 s/mm^2, 100 gradients) included a neurite orientation dispersion and density imaging (NODDI) model of intra-cellular volume fraction (ICVF), orientation dispersion index (ODI), and isotropic volume fraction (ISOVF). NODDI metrics were fit using the AMICO tool[18].

DWI metrics were projected to a standard white matter skeleton using publicly available ENIGMA protocols[19]. Briefly, each subject's whole-brain DTI-FA map was nonlinearly registered to the ENIGMA DTI-FA template using ANTs[20], and the resulting transformation was applied to the maps for each diffusivity metric. Diffusivity metrics were then projected onto the ENIGMA DTI-FA template skeleton using FSL's TBSS[21] and mean whole-skeleton diffusivity values were extracted for each metric.

2.3 Statistical analyses

Our primary analyses used linear regression models in R to examine the interaction between age and participant sex for each diffusivity metric (DTI-FA, TDF-FA, NODDI-ICVF, NODDI-ODI, NODDI-ISOVF). These models included mean-centered linear and quadratic age terms, sex, and the interaction between age and sex, as well as the following nuisance covariates[22]: educational attainment (operationalized as "college" or "no college"), socioeconomic status (quantified using the Townsend Deprivation Index[23]), waist-hip ratio, and population structure (measured using the first 4 principal components obtained from the UK Biobank's genetic ancestry analyses). We also completed supplementary analyses that included arterial stiffness (quantified using pulse wave velocity as a proxy for arterial blood pressure) as an additional nuisance covariate or body mass index (BMI) as a nuisance covariate instead of waist-hip ratio.

To assess the robustness of results, two additional statistical approaches were used: fractional polynomials and binarizing age into a discrete variable. Fractional polynomials allow continuous independent variables, such as age, to be flexibly modeled in a non-linear manner without specifying *a priori* the relationship between the independent and dependent

variable[24-26]. We used fractional polynomials to find the best-fitting model for age for each diffusivity metric (DTI-FA, TDF-FA, NODDI-ICVF, NODDI-ODI, NODDI-ISOVF) by testing one- and two-term curvilinear models for age using the following possible powers: -2, -1, -0.5, 0, 0.5, 1, 2 and 3, where x^0 corresponds to $ln(x)$; these analyses also included our covariates of non-interest (educational attainment, socioeconomic status, waist-hip ratio, population structure) and participant sex. After finding the best-fitting model for each diffusion measure, the interaction between age and sex was then tested for each measure using Stata's MFPI package[27]. To further assess the robustness of results to the chosen statistical model, we also followed previously published statistical recommendations[27] to repeat analyses after discretizing the continuous variable of interest. Specifically, we binarized age by splitting participants into two groups: $\geq$ 60 years old and < 60 years old; this binarization threshold was selected based on previous large-scale neuroimaging studies examining aging[25,26]. We then tested the interaction between age group and sex for each diffusivity metric using a linear regression model that also included the main effects of age group and sex, as well as our covariates of non-interest.

Lastly, sex-stratified normative centile reference curves[11-13] were created for each diffusivity metric using quantile regression to model age continuously with linear and quadratic age terms (Figure 1).

3. RESULTS

Our primary linear regression analyses revealed that significant sex differences in white matter aging were detected by advanced DWI metrics only. Specifically, a significant age by sex interaction was found for NODDI-ODI (linear age $p < 0.001$) and NODDI-ISOVF (linear age $p = 0.04$, quadratic age $p = 0.003$), with a marginally significant interaction found for TDF-FA (quadratic age $p = 0.059$). Sex differences in white matter aging were not significant for the traditional metric DTI-FA or for NODDI-ICVF (all ps > 0.2).

Supplemental analyses including arterial stiffness or BMI as nuisance covariates resulted in highly similar findings. The interaction between age and sex remained significant for NODDI-ODI (both linear age ps < 0.001) and NODDI-ISOVF (both linear age ps < 0.05; both quadratic age ps < 0.01), with the interaction also attaining statistical significance for TDF-FA (both quadratic age ps < 0.05). In line with our primary analyses, there were no significant group differences in aging between men and women on average for DTI-FA or NODDI-ICVF (all ps > 0.1).

When assessing the robustness of our primary results by using fractional polynomials to model age, we similarly found that sex differences in aging were detected by advanced DWI methods only. The interaction between age and participant sex was significant for NODDI-ODI ($p < 0.001$), as well as marginally significant for NODDI-ISOVF ($p = 0.053$). White matter aging did not significantly differ between male and female participants on average when using DTI-FA, TDF-FA, or NODDI-ICVF (all ps > 0.2).

In line with the results of our primary linear regression analyses, as well as those from our fractional polynomial analyses, follow-up exploratory analyses binarizing participants into two age groups ($\geq$ 60 years and < 60 years) similarly indicated significant interactions between age group and sex for advanced diffusivity metrics only. Specifically, age group by sex interactions were significant for NODDI-ODI ($p < 0.001$) and TDF-FA ($p = 0.02$), but not for DTI-FA, NODDI-ICVF, or NODDI-ISOVF (all ps > 0.1).

Normative centile reference curves for each metric, calculated using quantile regression, are presented in Figure 1 for male and female participants separately.

4. DISCUSSION

We found that advanced measures of white matter microstructure detected significant sex differences in aging in the UK Biobank, unlike traditional diffusivity metrics (DTI-FA). Specifically, NODDI-ODI demonstrated robust aging-related group differences between male and female participants on average. NODDI-ISOVF and TDF-FA also tended to exhibit aging-associated differences between men and women, although the exact pattern of findings for these metrics depended

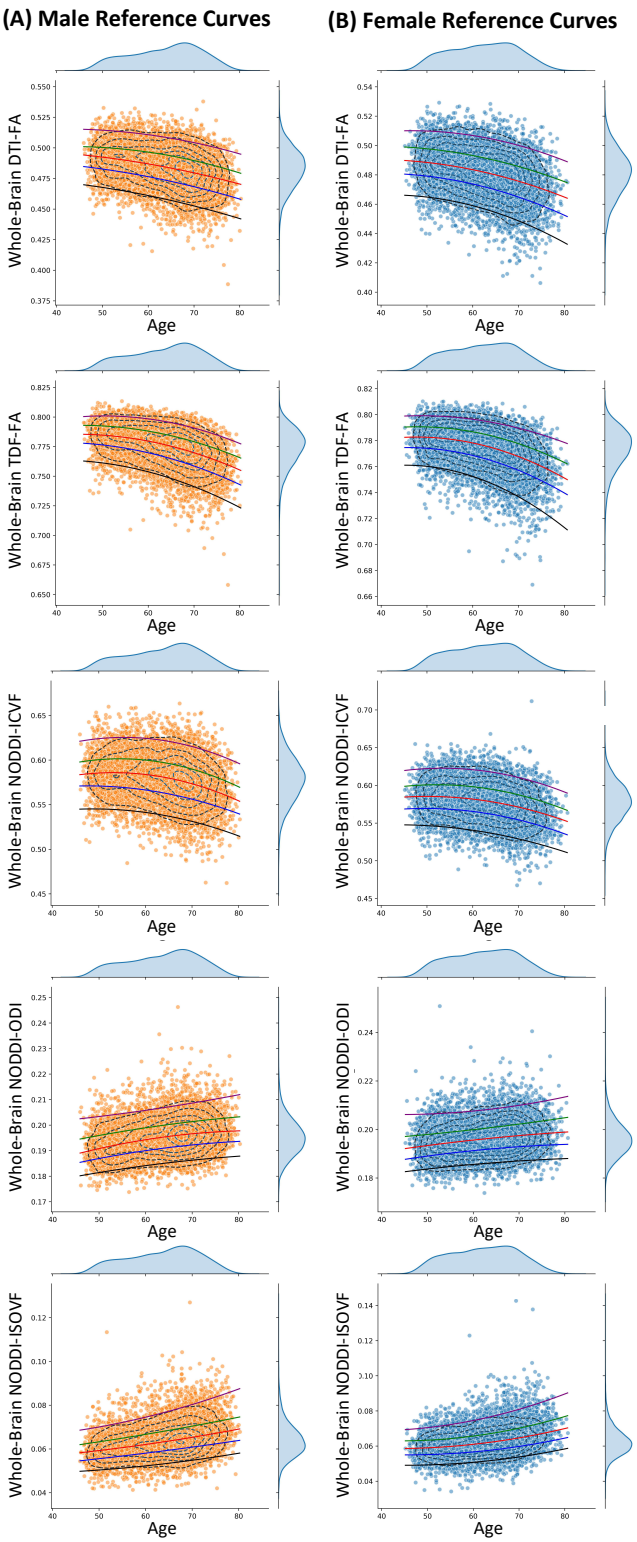

Figure 1. Normative centile reference curves calculated for each metric using quantile regression for (A) male participants, and (B) female participants Solid colored lines indicate the following centiles: 5th (black), 25th (blue), 50th (red), 75th (green), 95th (purple). Each dot represents one participant, with orange dots representing males and blue dots representing females. Dotted lines within each plot reflect data density, with distributions for each diffusivity metric and age presented as histograms to the top and right of each plot.

on the statistical approach used to model age. Notably, the traditional DWI metric, DTI-FA, consistently failed to capture sex differences in aging across all statistical approaches used.

NODDI fits a multi-compartment model to multi-shell DWI data to distinguish intra- and extra-cellular contributions to diffusion[10], resulting in metrics that may provide greater biological interpretability than metrics derived from single-shell DWI data, such as DTI-FA. This improved biological specificity of NODDI may contribute to our finding that NODDI-ODI and NODDI-ISOVF were particularly sensitive to sex differences in aging. For instance, our results indicate that measures of white matter dispersion (NODDI-ODI) exhibit sex differences in aging trajectories whereas measures of white matter density do not show detectable differences (NODDI-ICVF). As both of these underlying biological processes are thought to contribute to DTI-FA, this may explain why DTI-FA was less sensitive to aging differences between men and women than NODDI-ODI.

TDF is an advanced approach for single-shell DWI data which a fits a continuous distribution of tensors, whereas DTI fits a single-tensor model to single-shell DWI data[6,7]. As the brain's white matter includes crossing fibers, the model used by TDF may thus adhere more closely to the underlying biology than DTI[8]. This may contribute to our finding that TDF-FA was more sensitive to sex differences in aging than DTI-FA. However, TDF-FA was less sensitive to such sex differences than the multi-shell measure NODDI-ODI. As NODDI provides greater biological specificity than TDF-FA, together these findings suggest that models that align more closely with the brain's underlying biology may also provide greater sensitivity to aging-related sex differences. Additionally, compared to DTI-FA, TDF-FA may be well-suited for analyzing archival single-shell data.

We also created sex-stratified normative reference curves for each diffusivity metric. Such reference curves could have future clinical applications by allowing for the identification of individuals who may be at risk for age-related neurodegenerative diseases, such as Alzheimer's disease[11]. However, future longitudinal studies are needed to specifically assess the potential clinical utility of such reference curves for the current diffusivity metrics. Additionally, these age-dependent reference curves would need to be adjusted if applied to brain data coming from new scanners and cohorts. The error variance in the metrics shown here depends to some extent on the scanner, scan protocol, and hardware, such that the centile at which an individual appears in these reference curves would be biased unless their data had the same error variance as the single-scanner UK Biobank data from which these charts were derived. Many harmonization efforts are underway to allow cross-scanner transfer, which would allow the adaptation of these normative charts to data collected on different scanners within the UK Biobank, as well as data collected on new scanners elsewhere. These harmonization methods include ComBat[28] and its variants (ComBat-GAM[29], longitudinal ComBat[30], and CovBat[31]), hierarchical Bayesian models that model the mean, variance, and other moments of the cohort data[32], and transfer learning models. Additional approaches can be applied to harmonize the diffusion MRI data directly[33,34], and they deserve further study, as they may further sensitize and boost statistical power in analyses such as those presented in this paper.

5. CONCLUSIONS

As a whole, our findings demonstrate the utility of advanced diffusivity metrics when studying sex differences in aging. Future research examining sex differences in the brain's white matter in healthy and diseased aging may benefit from including advanced diffusion measures.

ACKNOWLEDGMENTS

This research was supported by the National Institutes of Health (award numbers R56AG058854, U54EB020403, R01AG059874, P41EB015922), and a grant from Biogen, Inc. The contents of this paper are solely the responsibility of the authors and do not necessarily represent the views of the funders.

REFERENCES

[1] Lockhart S. N. and DeCarli C., "Structural imaging measures of brain aging," Neuropsychol Rev 24(3), 271-289 (2014).
[2] Cox S. R., Ritchie S. J., Tucker-Drob E. M., et al., "Ageing and brain white matter structure in 3,513 UK Biobank participants," Nat Commun 7, 13629 (2016).

[3] Riedel B. C., Thompson P. M. and Brinton R. D., "Age, APOE and sex: Triad of risk of Alzheimer's disease," J Steroid Biochem Mol Biol 160, 134-147 (2016).
[4] Belloy M. E., Napolioni V. and Greicius M. D., "A Quarter Century of APOE and Alzheimer's Disease: Progress to Date and the Path Forward," Neuron 101(5), 820-838 (2019).
[5] Jones D. K., "Studying connections in the living human brain with diffusion MRI," Cortex 44(8), 936-952 (2008).
[6] Leow A. D., Zhu S., Zhan L., et al., "The tensor distribution function," Magn Reson Med 61(1), 205-214 (2009).
[7] Zhan L., Leow A. D., Zhu S., et al., "A novel measure of fractional anisotropy based on the tensor distribution function," Med Image Comput Comput Assist Interv 12(Pt 1), 845-852 (2009).
[8] Nir T. M., Jahanshad N., Villalon-Reina J. E., et al., "Fractional anisotropy derived from the diffusion tensor distribution function boosts power to detect Alzheimer's disease deficits," Magn Reson Med 78(6), 2322-2333 (2017).
[9] Villalon-Reina J. E., Ching C. R. K., Kothapalli D., D. S. and Nir T., "Alternative diffusion anisotropy measures for the investigation of white matter alterations in 22q11.2 deletion syndrome," Proc SPIE 10975, 1-13 (2018).
[10] Zhang H., Schneider T., Wheeler-Kingshott C. A. and Alexander D. C., "NODDI: practical in vivo neurite orientation dispersion and density imaging of the human brain," Neuroimage 61(4), 1000-1016 (2012).
[11] Nobis L., Manohar S. G., Smith S. M., et al., "Hippocampal volume across age: Nomograms derived from over 19,700 people in UK Biobank," Neuroimage Clin 23, 101904 (2019).
[12] Bethlehem R. A. I., Seidlitz J., Romero-Garcia R., Dumas G. and Lombardo M. V., "Normative age modelling of cortical thickness in autistic males," bioRxiv, 1-23 (2019).
[13] Lv J., Di Biase M., Cash R. F. H., et al., "Individual deviations from normative models of brain structure in a large cross-sectional schizophrenia cohort," 1-24 (2020).
[14] Miller K. L., Alfaro-Almagro F., Bangerter N. K., et al., "Multimodal population brain imaging in the UK Biobank prospective epidemiological study," Nat Neurosci 19(11), 1523-1536 (2016).
[15] Alfaro-Almagro F., Jenkinson M., Bangerter N. K., et al., "Image processing and Quality Control for the first 10,000 brain imaging datasets from UK Biobank," Neuroimage 166, 400-424 (2018).
[16] Andersson J. L. and Sotiropoulos S. N., "Non-parametric representation and prediction of single- and multi-shell diffusion-weighted MRI data using Gaussian processes," Neuroimage 122, 166-176 (2015).
[17] Andersson J. L. R. and Sotiropoulos S. N., "An integrated approach to correction for off-resonance effects and subject movement in diffusion MR imaging," Neuroimage 125, 1063-1078 (2016).
[18] Daducci A., Canales-Rodriguez E. J., Zhang H., Dyrby T. B., Alexander D. C. and Thiran J. P., "Accelerated Microstructure Imaging via Convex Optimization (AMICO) from diffusion MRI data," Neuroimage 105, 32-44 (2015).
[19] Jahanshad N., Kochunov P. V., Sprooten E., et al., "Multi-site genetic analysis of diffusion images and voxelwise heritability analysis: a pilot project of the ENIGMA-DTI working group," Neuroimage 81, 455-469 (2013).
[20] Avants B. B., Tustison N. J., Song G., Cook P. A., Klein A. and Gee J. C., "A reproducible evaluation of ANTs similarity metric performance in brain image registration," Neuroimage 54(3), 2033-2044 (2011).
[21] Smith S. M., Jenkinson M., Johansen-Berg H., et al., "Tract-based spatial statistics: voxelwise analysis of multi-subject diffusion data," Neuroimage 31(4), 1487-1505 (2006).
[22] Salminen L. E., Wilcox R. R., Zhu A. H., et al., "Altered Cortical Brain Structure and Increased Risk for Disease Seen Decades After Perinatal Exposure to Maternal Smoking: A Study of 9000 Adults in the UK Biobank," Cereb Cortex 29(12), 5217-5233 (2019).
[23] Townsend P., Phillimore P. and Beattie A., [Health and Deprivation: Inequality and the North], Routledge, (1988).
[24] Royston P. and Altman D., "Regression using fractional polynomials of continuous covariates: parsimonious parametric modelling," Applied Statistics 43(3), 429-467 (1994).
[25] Dima D., Papachristou E., Modabbernia A., Doucet G. E. and Agartz I., "Subcortical Volume Trajectories across the Lifespan: Data from 18,605 healthy individuals aged 3-90 years," bioRxiv, 1-28 (2020).
[26] Frangou S., Modabbernia A., Doucet G. E., et al., "Cortical Thickness Trajectories across the Lifespan: Data from 17,075 healthy individuals aged 3-90 years," bioRxiv, 1-35 (2020).
[27] Royston P. and Sauerbrei W., "A new approach to modelling interactions between treatment and continuous covariates in clinical trials by using fractional polynomials," Stat Med 23(16), 2509-2525 (2004).
[28] Fortin J. P., Parker D., Tunc B., et al., "Harmonization of multi-site diffusion tensor imaging data," Neuroimage 161, 149-170 (2017).
[29] Pomponio R., Erus G., Habes M., et al., "Harmonization of large MRI datasets for the analysis of brain imaging patterns throughout the lifespan," Neuroimage 208, 116450 (2020).

[30] Beer J. C., Tustison N. J., Cook P. A., et al., "Longitudinal ComBat: A method for harmonizing longitudinal multi-scanner imaging data," Neuroimage 220, 117129 (2020).
[31] Chen A. C., Beer J. C., Tustison N. J., Cook P. A., Shinohara R. T. and Shou H., "Removal of Scanner Effects in Covariance Improves Multivariate Pattern Analysis in Neuroimaging Data," bioRxiv, 1-20 (2019).
[32] Kia S. M., Huijsdens H., Dinga R., et al., "Hierarchical Bayesian Regression for Multi-Site Normative Modeling of Neuroimaging Data," arXiv, 1-12 (2020).
[33] Cetin Karayumak S., Bouix S., Ning L., et al., "Retrospective harmonization of multi-site diffusion MRI data acquired with different acquisition parameters," Neuroimage 184, 180-200 (2019).
[34] Moyer D., Ver Steeg G., Tax C. M. W. and Thompson P. M., "Scanner invariant representations for diffusion MRI harmonization," Magn Reson Med 84(4), 2174-2189 (2020).